Methods for fabricating Ohmic contacts to nanowires and nanotubes

E. Stern[a),b)]
Department of Biomedical Engineering, Yale University, P.O. Box 208284, New Haven, Connecticut 06520-8284

G. Cheng,[a),c)] J. F. Klemic, E. Broomfield, and D. Turner-Evans
Department of Electrical Engineering, Yale University, 15 Prospect Street, P.O. Box 208284, New Haven, Connecticut 06520-8284 and Department of Applied Physics, Yale University, 15 Prospect Street, P.O. Box 208284, New Haven, Connecticut 06520-8284

C. Li and C. Zhou
Department of Electrical Engineering-Electrophysics, University of Southern California, Building OHE 106 Mail Code 1455, University Park, Los Angeles, California 90089

M. A. Reed
Department of Electrical Engineering and Applied Physics, Yale University, 15 Prospect Street, P.O. Box 208284, New Haven, Connecticut 06520-8284 and Department of Applied Physics, Yale University, 15 Prospect Street, P.O. Box 208284, New Haven, Connecticut 06520-8284

(Received 9 September 2005; accepted 5 December 2005; published 19 January 2006)

A comparison of methods to create Ohmic contacts to semiconductor nanowires (NWs) and carbon nanotubes (CNTs) is presented. A Ni/Au lift-off metallization was used to contact GaN and In_2O_3 NWs and CNTs using electron-beam (e-beam) or optical lithography. In order to render the metal-semiconductor contacts Ohmic, e-beam-processed devices are found to require a postfabrication, high-temperature anneal, whereas the use of an oxygen plasma prior to metallization is found to be crucial for devices defined by optical lithography. © *2006 American Vacuum Society.* [DOI: 10.1116/1.2162575]

I. INTRODUCTION

Semiconducting nanowires (NWs) are a subject of intense contemporary interest because they represent the limit of semiconductor crystalline solids.[1,2] These structures are typically solid cylinders a few nanometers in diameter and multiple microns in length that are single crytal and can be forged from many semiconducting materials, including Si, GaN, GaAs, InN, and In_2O_3.[3,4] GaN is of particular interest because it has been shown to yield good quality wires and can be either as-grown *n* type or doped *p* type by the incorporation of magnesium during growth.[5,6] In_2O_3 is also of great interest because it has been shown to be promising for sensor applications.[7–9]

Unfortunately most as-grown NW processes are incompatible with electrical characterization of individual wires. Additional processing is thus required to remove the NWs from their growth substrate and deposit them onto a platform that permits the study of single wires. In order to characterize electronic transport in NWs it is necessary to define isolated contacts to individual NWs secured to leads, which is most readily achieved using microlithographic processing on a planar substrate. With this contacting method, the underlying substrate can also serve as an electrostatic gate, allowing for high throughput characterization of nanowire devices and material parameters.[10] Currently, there are few successful schemes for aligning NWs on the planar substrates,[11–14] thus electron-beam (e-beam) lithography is typically the method of choice for device fabrication because it allows a specific pattern to be written for each NW, assuring successful contacts will be created. A postmetallization anneal is typically employed prior to electrical testing to increase contact quality.[9,15] In this article we compare e-beam-fabricated NW devices with devices created with a high-throughput optical method and demonstrate that both schemes can be used to create Ohmic contacts to GaN NWs. We further show that the optical method is capable of contacting In_2O_3 NWs and carbon nanotubes (CNTs).

II. EXPERIMENTAL METHODS

A. Nanowire samples

The GaN NWs used for this study were grown by the vapor-liquid-solid (VLS) technique in a hot-wall chemical-vapor deposition (CVD) system. The NWs were grown on an alumina template with a 20 Å-thick nickel catalyst deposited using an e-beam evaporator. When heated, the thin metal film coalesces into molten nanoparticles, each of which serves as a growth catalyst for a single NW. Gallium from a solid source and nitrogen produced by the cracking of ammonia dissolve into the metal and crystal growth is nucleated at the substrate and proceeds upwards, Fig. 1. Previous studies have shown that these wires are single crystal and that their diameters are dependent on the size of the metal catalyst particles.[10] When growth is complete, the NWs strongly adhere to the substrate, which is removed from the furnace for further processing. Samples from five growths used in this article are outlined in Table I. A mixture of elemental Ga

[a)]Authors to whom correspondence should be addressed.
[b)]Electronic mail: eric.stern@yale.edu
[c)]Electronic mail: guosheng.cheng@yale.edu

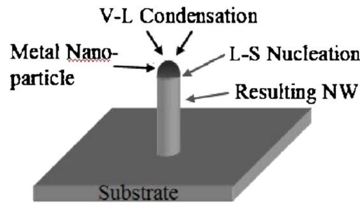

FIG. 1. Schematic depicting VLS growth. Gallium and ammonia vapor condense in the molten nickel nanoparticle, VL condensation, and crystallize at the substrate, LS nucleation.

and its oxide is used as the gallium source because it has been found to produce a higher NW yield.[10] Other studies performed have found that the growth conditions of all three growths outlined above yield wires with a carrier concentration of $\sim 1 \times 10^{20}$ cm^{-3}, thus all NWs are in the near-degenerate doping region.

Indium oxide NWs were also fabricated into devices because these NWs have been shown to be nondegenerately doped, with carrier concentrations between $\sim 10^{16} - 10^{18}$ cm^{-3}.[8] These wires were grown by the laser-ablation method, which has been described previously.[8]

Carbon nanotubes were obtained from a commercial source, Tubes @ Rice, Inc. No effort was made to separate metallic from semiconducting devices; thus a random sampling of semiconducting and metallic, single- and multiwall CNTs is expected.[16] The presence of all CNT types is corroborated by a two-order-of-magnitude variance in resistance across CNT devices, from $\sim 10^4 - 10^6$ Ω, and by the strong gating dependencies of some devices.

B. Lithographic processing

The processing steps for both the e-beam and optical processes are outlined in Fig. 2. Starting with a 2-in. $p^{++}(10^{19}$ cm$^{-3})$ boron-doped silicon wafer with a 200 nm thermal oxide (Silicon Quest International), vias are defined through the oxide to create topside contacts to the backgate with wet chemical etching using 6:1 buffered hydrofluoric acid. All chemicals were purchased from MicroChem, Inc. and are complementary metal-oxide semiconductor (CMOS) grade. A positive photoresist, S1813 (Shipley), is used to define the via pattern and after exposure (using an EV Group

TABLE I. Table showing the growth conditions varied for GaN NW samples used in this study. For all samples, the catalyst was Ni, the pressure was ~760 Torr, the NH_3 flux was 100 SCCM (standard cubic centimeter per minute), and the gallium source was a mixture of elemental gallium and gallium oxide.

Growth	Substrate	Temp (°C)
A	Alumina	840
B	Alumina	850
C	Silicon	900
D	Silicon	1000
E	Silicon	1100

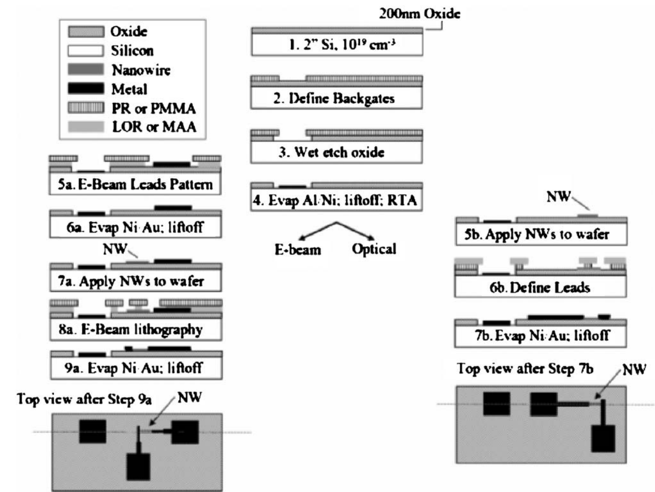

FIG. 2. Schematic of the process flows. Steps 1–4 illustrate backgate definition; steps 5a–9a show the e-beam contacting process while steps 5b–7b depict the optical contacting process. The horizontal and vertical dimensions are not to scale.

620) and development (using a 1:1 dilution of MF312: deionized water), the wafer is etched in a 6:1 buffered hydrofluoric acid and metallized with 50 nm Al (99.999%, Kurt J. Lesker Co.)/ 10 nm Ni (99.995%, Kurt J. Lesker Co.). Liftoff is subsequently performed in acetone with sonication. The wafers are then rapid-thermal annealed at 300 °C for 30 s with a HeatPulse 210T-02 to ensure the backgate (substrate) contacts are Ohmic. Although backgated devices are not critical to the characterization discussed in this article, contacting the backgate allows for eventual fabrication of a NW-based field-effect transistor (FET).

For direct write electron-beam lithography, an additional optical lithographic processing step is used to define leads from contact pads to an 80 μm^2 e-beam writing window, including e-beam alignment marks within this window. In order to minimize flagging of the lift-off metallization, a resist bilayer consisting of a lift-off resist (LOR), (MicroChem), that develops anisotropically, and a photoresist (S1813) is used (Fig. 2, step 5a). Thus when a LOR/S1813 stack is created (Fig. 2, step 6b), the undercut of the LOR can be carefully controlled and an ideal lif-toff profile is created. A 10 nm Ti (99.995%, Kurt J. Lesker)/ 200 nm Au (99.999%, Cerac Inc.) stack is e-beam evaporated and lift-off is achieved in 60 °C 1-methyl-2-pyrrilidinone (NMP) with sonication (Fig. 2, step 6a). Although it is possible to write contact pads directly using e-beam lithography for individual NW devices, it is not practical for producing large numbers of devices with four or more contacts, required to eliminate contact resistance.

The NWs are then transferred from their growth substrate by suspending them in isopropanol (IPA), which is achieved by briefly sonicating the growth substrate in alcohol for 10–45 s. The suspension is then is applied dropwise to the wafer (Fig. 2, step 7a) and upon IPA evaporation NWs adhere to the oxide surface in a random dispersion across the wafer. The NWs have been found to strongly adhere to the

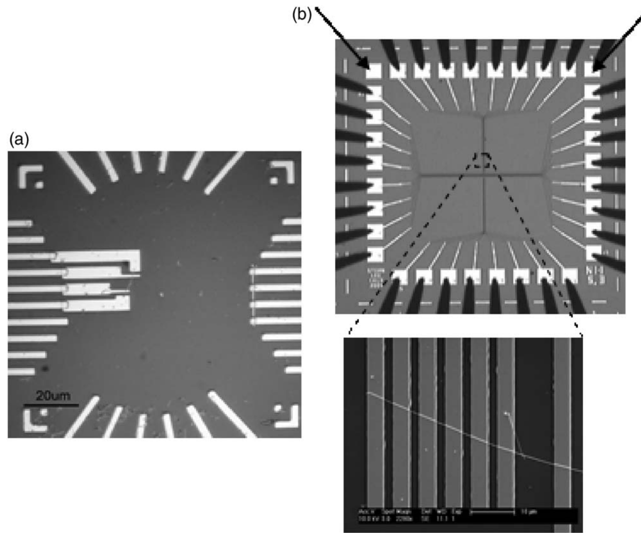

FIG. 3. (a) Representative four-point contact to a GaN NW defined by e-beam lithography. Optically defined lead-ins and alignment marks are seen to provide fan-outs and window definition, respectively, for the e-beam-defined contacts. At the right of the micrograph is an e-beam-defined lithographic short. (b) Optical micrograph of a typical 3.333 mm^2 die with a FESEM inset magnification of a GaN NW contacted with seven metal leads. The black arrows denote the pads contacting the backgate. The die is shown contacted by 33 probetips of a Cascade Microsystems Autoprobestation, used for automated device screening.

wafer; sonication and etching are the only successful removal methods. The writing windows are canvassed using an optical microscope (a scanning electron microscope could also be used) until the desired number of e-beam windows contain NWs. This dispersion method is relatively insensitive to growth yield because of the deposition/screening iterations and because wires lying in any orientation in the e-beam window can be contacted.

After NW deposition, a MAA EL 13 MAA / PMMA 950 A4 (MicroChem) bilayer is spun on the wafer and an optical image is taken of each writing window. Alternatively, a scanning electron microscopy (SEM) image can be taken before resist spinning and it has been found that the location of the NWs on the wafer surface is largely unaffected by the resist application. Patterns are then created to define leads to each NW device with a JEOL 6400 SEM converted to perform direct write. The resist is exposed using typical electron doses of 350 $\mu C/cm^2$, and a 1:3 mixture of methyl isobutyl ketone (MIBK, MicroChem):IPA is used for development (Fig. 2, step 8a). A 50 nm Ni/300 nm Au e-beam evaporation is then performed using boiling acetone for the lift-off (Fig. 2, step 9a). Ni is used because it has been shown to make Ohmic contacts to n-type GaN NWs;[6] gold is used because of its high conductivity and ease of wirebonding. A typical device is shown in Fig. 3(a).

In the optical processing method, NWs are dispersed by the technique described above after backgate processing is completed (Fig. 2, step 5b). A subsequent optical step is then performed to create metal contacts to the NWs that fan out to contact pads. Photolithography is then used to pattern lines 2 or 3 μm in width and spaced 2 or 3 μm apart, respectively, that run parallel for $\sim$1 mm before fanning out to contact pads and this step is followed by a metal deposition. Adjacent metal leads are electrically isolated unless linked by a NW. Two limitations to the optical contacting method can be seen at this point: the wires must be at least $\sim$3 μm long (ideally $>$5 μm) to span the leads and the NW density must be high in order to obtain devices since the leads cover 1.6% or 2.4% of the chip's area for the 2 and 3 μm patterns, respectively. Samples with low NW yields can sometimes be successfully fabricated by applying multiple drops of the NW suspension to the wafer but a certain density threshold must be met in order to obtain devices. The NW density must also be sufficiently low such that the majority of devices are due to an individual wire; thus the density must be carefully chosen to lie within these boundaries.

A lift-off metallization of the contacts must be performed because subjecting the NWs to metal etchants could be detrimental to their properties since their stability is unknown. Furthermore, sonication cannot be used to clean the wafers or to aid the lift-off because it may remove NWs from the wafer. Again, a LOR/S1813 bilayer is used to create the necessary lift-off profile. A 50 nm Ni/200 nm Au stack is then evaporated with an e-beam evaporator (same equipment and procedure as in the e-beam lithography process) and lift-off is achieved in NMP at 60 °C without sonication, creating the contacts to the NWs (Fig. 2, step 7b), as pictured in Fig. 3(b).

C. Device characterization

All electrical measurements were performed with an HP4156B semiconductor parameter analyzer (SPA). Two-point measurements were taken by varying the voltage and measuring current; four-point measurements were taken by sweeping a current across the outer leads and measuring the voltage across the inner leads. Two-point measurements were taken for the inner electrodes of the four-point contact and resistance values are defined as the zero-bias slope.

Samples processed with e-beam lithography were measured on a manual probestation with Cascade Microtech probes; for the optical process, a Cascade Microtech autoprobe station was used to step die by die and electrically screen all adjacent contact leads across the entire wafer of $\sim$150 dies for NW crossings, Fig. 3(b). An Agilent Technologies switchbox was used to multiplex the Cascade system for the optical process samples. Leads with Ohmic contacts to NWs were imaged with a field-emission scanning electron microscopy (FESEM) to ensure that each lead pair contacted a single NW; data from lead pairs with multiple parallel NWs are discarded.

III. RESULTS AND DISCUSSION

Nanowire contacts for the GaN devices fabricated as described have resistances varying over two orders of magnitude, from $\sim$35 kΩ to $\sim$5.4 MΩ. Four-point measurements that eliminate contact resistance show that this wide dispersion in resistance values is caused by the variance in NW diameters (which range from 25 to 300 nm) and in doping density.[10] The three growths outlined above have all been

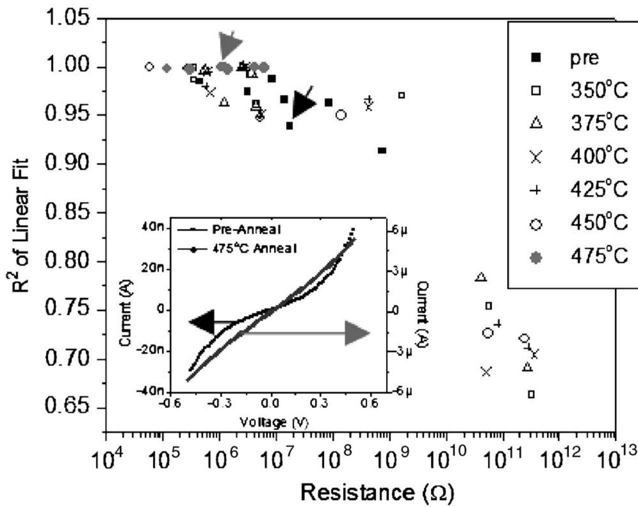

FIG. 4. Scatter plot of the R^2 value of a linear best-fit line to the inverse of the $I(V)$ two-point data vs the slope of this best-fit line (resistance) for e-beam-processed samples. Data points are shown for unannealed samples as well as six 1 min anneals in 25 °C increments from 350 to 475 °C for seven samples. Preannealed data points are solid squares and post-475 °C-annealed data points are solid circles. The inset plot shows a −0.5 to 0.5 V current-voltage sweep for a characteristic device; the preanneal and post-475 °C-annealed data points for this device are arrowed. The left-hand axis of the inset plot shows the sweep before annealing and the right-hand one the device after the 475 °C anneal, which is seen to be approximately two orders of magnitude more conductive than the unannealed sample.

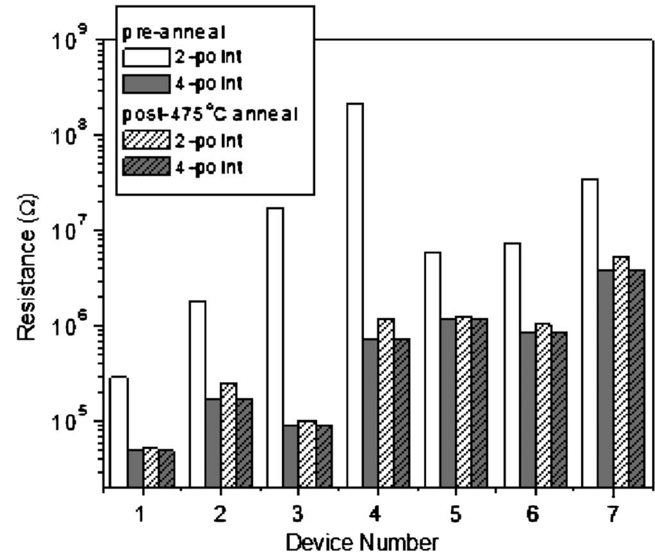

FIG. 5. Comparison of two- and four-point resistances of pre- and post-475 °C-annealed devices. For annealed devices, the difference between two-point and four-point resistances is never greater than 19.7% of the wire resistance. Device 3 is the "characteristic" device highlighted in Fig. 4.

found to yield wires with carrier concentrations $\sim 1 \times 10^{20}$ cm^{-3}, thus all NWs are in the degenerate doping region.[10] Ohmic contacts are defined as devices with the best-fit line to the $I(V)$ plot having a correlation coefficient $R^2 > 0.99$ for $V = -1$ to 1 V. Data from 7 e-beam-defined four-point devices and from 206 two-point and 51 four-point optically devices are presented for GaN NWs, as well as data from 60 In_2O_3 NWs and 60 CNTs. Nanowires from growth A were used for the e-beam devices; NWs from growths A and B were used for two-point optically defined devices and those from growths C–E produced optical four-point devices.

E-beam-processed NW devices were found to repeatedly produce contacts with apparent Schottky barriers of varying heights and, consequently, linear best fits to the two-point $I(V)$ characteristics of these devices routinely yield $R^2 < 0.975$ (Fig. 4). A $I(V)$ characteristic of a representative device is shown in the left-hand curve in the inset plot in Fig. 4 (for a later reference, device 3 in Fig. 5). The preanneal and post-475 °C-anneal data points in Fig. 4 for this device are highlighted by arrows. The seven devices plotted in Fig. 5 are each contacted by four leads and a comparison of the resistances given by two-point and 4-point measurements shows the dominance of the contact resistance in e-beam-preannealed devices. On average for these seven samples, only 9.6% of the two-point resistance of these seven samples is due to the NW itself.

Annealing metal-bulk GaN contacts has been shown to decrease the contact resistance;[17] in order to study the effects of different annealing temperatures on the contact resistance the samples were annealed on a hot plate in a N_2 environment for 1 min at 25 °C increments from 350 to 475 °C. Samples were immediately transferred to a thermal sink after each anneal and two-point and four-point measurements were subsequently taken. The two-point resistances and corresponding R^2 values of the linear fit are shown for each temperature in Fig. 4. The right-hand curve in the inset plot shows the post-475 °C-anneal two-point IV sweep for device 3 in Fig. 5. It is interesting to note that some devices became significantly more resistive and nonlinear after intermediate annealing temperatures before reaching their final low-resistance, linear states at higher annealing temperatures. It has been found that the 1 min 475 °C anneal alone (without lower-temperature anneals) renders devices Ohmic. Over 50 NW devices have been fabricated by the e-beam process and ~95% have been found to survive the postprocessing annealing step.

Optically fabricated devices were also found to have contacts with Schottky barriers, exemplified by the data set of 104 devices with low R^2 linear fit values in Fig. 6. The nonlinear nature of the $I(V)$ sweeps is shown on the right-hand axis in the inset plot for a characteristic device, denoted by an arrow in Fig. 6. We hypothesized that resist residue remaining on the NWs after development was responsible for the nonlinear electrical behavior of the contacts. To eliminate this problem, a GaSonics Aura 2000 Asher was used to perform a 20 s postdevelopment, premetallization descum in an oxygen plasma with 4 SLPM (standard liters per minute) O_2 at 100 mTorr and 25 °C. The vast majority of the 102 devices obtained from this process and plotted here have linear $I(V)$ characteristics and lower resistances than the devices not subjected to the oxygen plasma, Fig. 6. A characteristic device is denoted by an arrow and the $I(V)$ plot is shown in the inset. We observe that the postfabrication annealing pro-

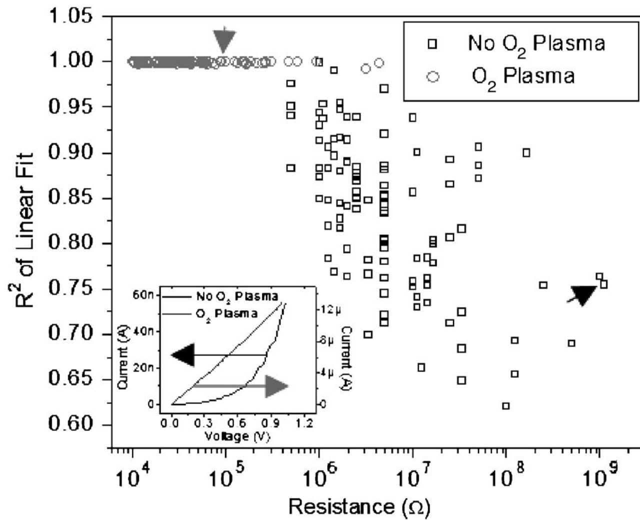

FIG. 6. Scatter plot of the R^2 value of a linear best-fit line to the inverse of the I vs V two-point data vs the slope of this best-fit line (resistance) for optically processed samples. Data points from samples not subjected to the oxygen plasma are shown as squares; the circles illustrate samples descummed with the plasma. The inset plot shows a 0–1 V current-voltage sweep for two characteristic devices circled with dotted lines in the scatter plot. The right-hand axis of the inset plot shows the sweep of the non-oxygen-plasma-treated device and the left-hand one shows the oxygen plasma-treated device, which is seen to be approximately two orders of magnitude more conductive than the untreated device. There are 206 total data points.

tocol developed for e-beam-processed devices did not produce Ohmic contacts for optical devices without oxygen plasma treatment and often destroyed devices. Additionally, we observe that the use of an identical oxygen plasma protocol on e-beam-defined samples is ineffective (e.g., contacts are initially Schottky and require subsequent anneals in order to be made Ohmic).

For 51 optical samples contacted by four or more leads, the two-point resistances are found to lie within an average of 4.9% of their four-point counterparts, Fig. 7. This indicates that the linear fit $R^2 > 0.99$ values to the $I(V)$ curves of the oxygen plasma-treated samples correspond to minimal metal-semiconductor contact resistances.

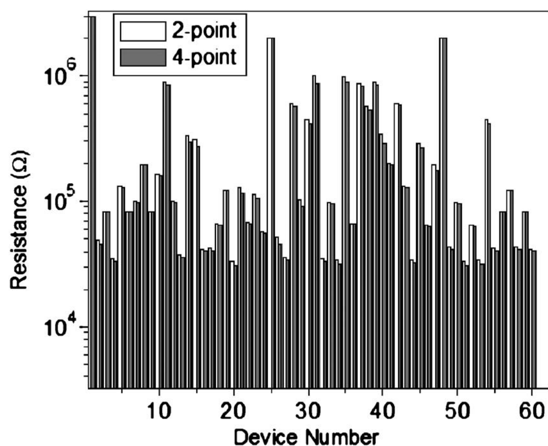

FIG. 7. Two- and four-point resistances of 60 unannealed devices defined by optical lithography with oxygen plasma prior to metallizing. The contact resistance is seen to be minimal.

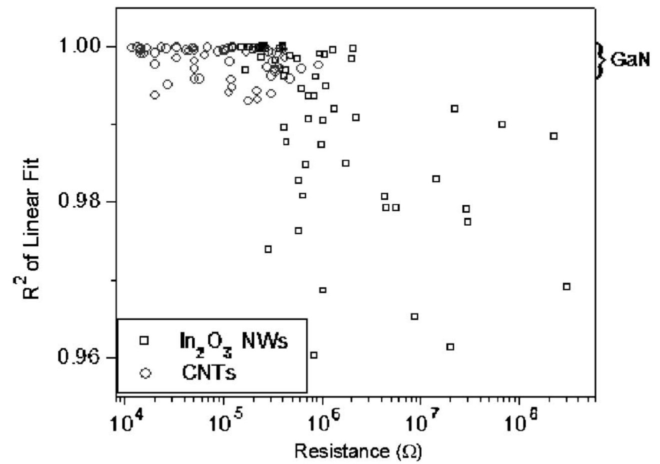

FIG. 8. Scatter plot of the R^2 value of a linear best-fit line to the inverse of the I vs V two-point data vs the slope of this best-fit line (resistance) for optically processed samples of In_2O_3 and CNTs. Data points from In_2O_3 NWs are squares and those from CNTs are circles. There are 60 data points from In_2O_3 NWs and 60 from CNTs. The bracket on the right of the plot shows the range of oxygen-plasma-processed GaN R^2 values from Fig. 6.

Furthermore, optical processing with the premetallization oxygen plasma treatment has been successfully employed to create Ohmic contacts to nondegenerately doped In_2O_3 NWs as well as to CNTs (Fig. 8). The plot shows data from 60 In_2O_3 NWs and 60 CNTs. Sixty-two percent of the In_2O_3 NWs have a linear fit $R^2 > 0.99$ and all CNTs have a linear fit $R^2 > 0.99$. The figure illustrates that the same processing method can be used to create Ohmic contacts to degenerate and nondegenerate NWs as well as metallic and semiconducting CNTs.

IV. CONCLUSION

This work shows that Ni/Au leads defined by either optical or e-beam lithography can ohmically contact GaN NWs. On optical lithographically processed samples, an oxygen plasma clean prior to metallization is critical for producing Ohmic contacts (samples not subjected to cleaning had Schottky contacts), implying that residual resist is effectively removed by the plasma clean. In contrast, devices processed with e-beam lithographically yield Schottky contacts regardless of oxygen plasma cleaning, suggesting that the electron beam produces surface damage resulting in Fermi-level pinning of the NW. A subsequent high-temperature anneal converts these Schottky contacts to Ohmics with nominally equivalent specific contact resitivities to those of optically defined and oxygen plasma-treated devices.[18]

Electron-beam lithography is often the method of choice for contacting NWs and CNTs due to the ease of registration; however, the results of the current study imply that the electron beam can modify the intrinsic properties of the NW. In contrast, the optical lithographic process does not appear to introduce comparable surface modifications. Furthermore,

optical lithography offers significantly higher throughput and is capable of producing the statistically significant numbers of NW/CNT devices required to characterize intrinsic NW/CNT properties due to the prevalence of device-to-device fluctuations at the nanoscale. In addition, this method does not introduce systematic errors by preselecting devices.

ACKNOWLEDGMENTS

The authors would like to thank Dr. James Hyland, Dr. Michael Young, Dr. Robert Koudelka, Dr. Thomas Boone, Dr. Ilona Kretzschmar, Dr. Luigi Frunzio, and Matthew Reese for help with fabrication; Dr. Jia Chen (IBM) for assistance with CNT processing; Dr. Elena Cimpoiasu, Ryan Munden, and Aric Sanders for aid with the measurement setup; Dr. Ling Xie and John Tsakirgis for assistance with ashing at the Harvard NNIN cleanroom; Nick Bernardo and Vincent Bernardo for machining assistance; and Dr. Zhenting Jiang for aiding the FESEM work. This work was partially supported by DARPA through AFOSR, ARO (DAAD19-01-1-0592), AFOSR (F49620-01-1-0358), NASA (NCC 2-1363), by a Department of Homeland Security graduate fellowship, and by a NSF graduate fellowship.

[1]R. S. Wagner, in *Whisker Technology*, edited by A. P. Levitt (Wiley, New York, 1970), pp. 47–109.
[2]K. Hiruma, M. Yazawa, T. Katsuyama, K. Ogawa, K. Haraguchi, M. Koguchi, and H. Kakibayashi, J. Appl. Phys. **77**, 447 (1995).
[3]C. N. R. Rao, F. L. Deepak, G. Gundiah, and A. Govindaraj, Prog. Solid State Chem. **31**, 5 (2003).
[4]Y. Xia, P. Yang, Y. Sun, Y. Wu, B. Mayers, B. Gates, Y. Yin, F. Kim, and H. Yan, Adv. Mater. (Weinheim, Ger.) **15**, 353 (2003).
[5]W. S. Shi, Y. F. Zheng, N. Wang, C. S. Lee, and S. T. Lee, Adv. Mater. (Weinheim, Ger.) **13**, 591 (2001).
[6]G. Cheng, A. Kolmakov, Y. Zhang, M. Moskovits, R. Munden, M. A. Reed, G. Wang, D. Moses, and J. P. Zhang, Appl. Phys. Lett. **83**, 1578 (2003).
[7]C. Li, D. Zhang, S. Han, X. Liu, T. Tang, and C. Zhou, Adv. Mater. (Weinheim, Ger.) **15**, 143 (2003).
[8]C. Li, D. Zhang, X. Liu, S. Han, T. Tang, J. Han, and C. Zhou, Appl. Phys. Lett. **82**, 1613 (2003).
[9]Y. Cui, Q. Wei, H. Park, and C. M. Lieber, Science **293**, 533 (2001).
[10]E. Stern, G. Cheng, E. Cimpoiasu, R. Klie, S. Guthrie, J. Klemic, I. Kretzschmar, E. Steinlauf, D. Turner-Evans, E. Broomfield, J. Hyland, R. Koudelka, T. Boone, M. Young, A. Sanders, R. Munden, T. Lee, D. Routenberg, and M. A. Reed, Nanotech. **16**, 2941 (2005).
[11]D. Wang, S. Jin, Y. Wu, and C. M. Lieber, Nano Lett. **3**, 1255 (2003).
[12]T. Martensson, P. Carlberg, M. Borgstrom, L. Montelius, W. Seifert, and L. Samuelson, Nano Lett. **4**, 699 (2004).
[13]W. Salaha and E. Zussman, Phys. Fluids **17**, 063301 (2005).
[14]O. Englander, D. Christensen, J. Kim, L. W. Lin, and S. J. S. Morris, Nano Lett. **5**, 705 (2005).
[15]D. Wang, J. G. Lu, C. Jones-Otten, and W. E. Buhro, Appl. Phys. Lett. **83**, 5280 (2005).
[16]T. W. Odom, J.-L Huang, P. Kim, and C. M. Lieber, Nature (London) **391**, 62 (1998).
[17]S. Pal and T. Sugino, Appl. Surf. Sci. **161**, 263 (2000).
[18]E. Stern, G. Cheng, M. P. Young, and M. A. Reed (in press).